

Liquids tend to run off instead of remaining on the surface. Maintaining consistent contact with uneven surfaces using a liquid medium presents certain challenges due to the inherent properties of liquids, which tend to flow off rather than remain adhered to the surface. While several studies have investigated the use of water as a coupling medium, this approach has its limitations, notably the complexity it introduces into the surgical preparation process.<sup>5,6</sup> Despite these hurdles, our research has discovered that a solid gel can serve as an effective coupling medium for scanning purposes. This gel pad facilitates the transmission of ultrasound frequencies from the handpiece to the target tissue, enabling unrestricted movement during treatment.<sup>4,7</sup> With its potential to enhance ultrasound image quality, expand examination capabilities for irregular surface anatomy, and promote efficient ultrasound propagation in soft tissue, the gel pad shows promising potential as a tool to aid surgical procedures.

Nasal bone fractures constitute a substantial proportion of facial bone fractures, accounting for 40% to 50% of all facial bone fractures, with zygomatic fractures ranking next in frequency. These fractures have the potential to cause significant cosmetic and functional deformities. The reduction of the nasal bone and zygomatic arch fractures typically entails closed reduction, a process that hinges significantly on the surgeon's technique and experience. Concurrently, to circumvent the limitations concomitant with this blind technique, numerous surgeons have incorporated the use of intraoperative ultrasound, as supported by previous studies.<sup>2,3,8</sup> Nevertheless, the complex 3-dimensional curvature of the nose and zygomatic arch presents challenges when scanning the adjacent facial bones. We applied a solid gel pad to augment the visualization of ultrasound images during surgery, thereby granting the surgeon better visual feedback and real-time video monitoring. This enhancement has proven to markedly improve the quality of facial fracture surgeries, leading to superior patient outcomes.

In conclusion, the use of a solid gel pad as a coupling medium in ultrasonography for facial bone fractures greatly improves imaging quality. Intraoperative ultrasonography, when used with a coupling medium, facilitates the confirmation of fracture patterns, and enables a more precise closed reduction during blind techniques for facial bone fractures.

## REFERENCES

1. Suh MK. *State of the Art Rhinoplasty Techniques: Perspectives from Korean Masters*. Springer Nature; 2022
2. Abu-Samra M, Selmi G, Mansy H, et al. Role of intra-operative ultrasound-guided reduction of nasal bone fracture in patient satisfaction and patient nasal profile (a randomized clinical trial). *Eur Arch Oto-Rhino-Laryngol* 2011;268:541–546
3. Hwang S-M, Pan H-C, Kim H-I, et al. Reduction of nasal bone fracture using ultrasound imaging during surgery. *Arch Craniofac Surg* 2016;17:14
4. Tsui BC, Tsui J. A flexible gel pad as an effective medium for scanning irregular surface anatomy. *Can J Anaesth* 2012;59: 226–227
5. Shigemura Y, Ueda K, Akamatsu J, et al. Ultrasonographic images of nasal bone fractures with water used as the coupling medium. *Plast Reconstr Surg Glob Open* 2017;5:e1350
6. Shigemura Y, Akamatsu J, Sugita N, et al. Water can make the clearest ultrasonographic image during reduction of nasal fracture. *Plast Reconstr Surg Glob Open* 2014;2:e203
7. Corvino A, Sandomenico F, Corvino F, et al. Utility of a gel stand-off pad in the detection of Doppler signal on focal nodular lesions of the skin. *J Ultrasound* 2020;23:45–53
8. Yabe T, Tsuda T, Hirose S, et al. Comparison of ultrasonography-assisted closed reduction with conventional closed reduction for the treatment of acute nasal fractures. *J Plast Reconstr Aesthet Surg* 2014;67:1387–1392

OPEN

## Deletion of cis-regulatory Element in *FOXL2* Promoter in a Chinese Family of Type II Blepharophimosis-ptosis-epicanthus Inversus Syndrome with Polydactyly

Qin Shen, MD,\*† Xiaojun Zhao,\*† Yongrong Ji, MD,\*† and Peiwei Chai, PhD, MD\*†

From the \*Department of Ophthalmology, Ninth People's Hospital, Shanghai Jiao Tong University School of Medicine, Shanghai, People's Republic of China; and †Shanghai Key Laboratory of Orbital Diseases and Ocular Oncology, Shanghai, People's Republic of China.

Received July 31, 2023.

Accepted for publication August 26, 2023.

Address correspondence and reprint requests to Yongrong Ji, (e-mail: jyrjyr@163.com) and Peiwei Chai, PhD, MD, (e-mail: chaipeiwei123@sjtu.edu.cn), Department of Ophthalmology, Ninth People's Hospital, Shanghai Jiao Tong University School of Medicine, Shanghai, 200025, People's Republic of China.

Q.S. and X.Z. contributed equally to this work.

The whole exome sequencing has been deposited in the National Omics Data Encyclopedia (NODE, <https://www.biosino.org/>, OER422653).

Ethics approval for this study was obtained from Shanghai Jiaotong University. Only non-identifiable information is presented. The patient provided signed informed consent for an Institutional Review Board-approved protocol for research use of medical records, of pathologic specimens obtained as part of routine clinical care, and publication.

Written informed consent to publish the clinical data was obtained from the BPES family before the initiation of the study.

P.W.C., Y.R.J., and Q.S. planned the project. Q.S. and X.W.Z. designed the experiments. P.W.C. conducted the experiments. P.W.C., Y.R.J., and Q.S. collected clinical information and clinical samples. Q.S. and Y.R.J. analyzed the data. All authors wrote the paper. All authors discussed the results and commented on the manuscript.

This work was supported by National Natural Science Foundation of China (82103240) and Shanghai Science and Technology Innovation Action Plan (23ZR1480100).

The authors have no conflicts of interests to declare.

**Supplemental Digital Content is available for this article. Direct URL citations are provided in the HTML and PDF versions of this article on the journal's website, [www.jcraniofacialsurgery.com](http://www.jcraniofacialsurgery.com).**

This is an open access article distributed under the terms of the Creative Commons Attribution-Non Commercial-No Derivatives License 4.0 (CCBY-NC-ND), where it is permissible to download and share the work provided it is properly cited. The work cannot be changed in any way or used commercially without permission from the journal.

Copyright © 2023 The Author(s). Published by Wolters Kluwer Health, Inc. on behalf of Mutaz B. Habal, MD.

ISSN: 1049-2275

DOI: 10.1097/SCS.00000000000009801

**Abstract:** Blepharophimosis-ptosis-epicanthus inversus syndrome (BPES) is a relatively uncommon autosomal-dominant genetic disorder, primarily attributed to mutations in the forkhead box L2 (FOXL2) gene. Albeit the involvement of protein-coding regions of FOXL2 has been observed in the majority of BPES cases, whether deficiencies in regulatory elements lead to the pathogenesis remains poorly understood. Herein, an autosomal-dominant BPES type II family was included. Peripheral venous blood has been collected, and genomic DNA has been extracted from leukocytes. A whole exome sequencing analysis has been performed and analyzed (Deposited in NODE database: OER422653). The promoter region of FOXL2 was amplified using polymerase chain reaction (PCR). The luciferase reporter assay was performed to identify the activity of this region. In this study, we present a Chinese family diagnosed with type II BPES, characterized by the presence of small palpebral fissures, ptosis, telecanthus, and epicanthus inversus. Notably, all male individuals within the family display polydactyly. A 225-bp deletion in the 556-bp 5'-upstream to transcription start site of *FOXL2*, decorated by multiple histone modifications, was identified in affected members of the family. This deletion significantly decreased FOXL2 promoter activity, as measured by the luciferase assay. Conclusively, a novel 255-bp-deletion of the FOXL2 promoter was identified in Chinese families with BPES. Our results expand the spectrum of known FOXL2 mutations and provide additional insight into the genotype-phenotype relationships of the BPES pathogenesis. In addition, this study indicates the important role of genetic screening of cis-regulatory elements in testing heritable diseases.

**Key Words:** Blepharophimosis-ptosis-epicanthus inversus syndrome, *FOXL2*, mutations, polydactyly

Blepharophimosis, ptosis, and epicanthus inversus Syndrome (BPES) is an autosomal-dominant disease that affects the eyelids.<sup>1,2</sup> If left untreated, these characteristics are correlated with a high prevalence of amblyopia.<sup>3</sup> The diagnosis of BPES can be categorized into 2 types: type I BPES exhibits classic facial features and is linked to premature ovarian failure, while type II solely manifests with classic eyelid malformation.<sup>4-6</sup> It is noteworthy that in the majority of cases, both types of BPES are caused by mutations in the coding region of FOXL2 (OMIM #605597), a gene responsible for encoding a forkhead transcription factor.<sup>7</sup>

FOXL2, located on chromosome 3q23, is a single exon spanning 2.7 kb and encodes 376 amino acids. This includes a DNA-binding sequence and a poly-Ala tract.<sup>3</sup> It is noteworthy that poly-Ala expansion mutations often lead to BPES type II, while truncations before the poly-Ala tract commonly result in the pathogenesis of BPES type I.<sup>8</sup> Various tissues, such as granulosa cells in the ovary, the mesenchyme of the developing eyelid, and gonadotropic cells in the anterior pituitary, exhibit significant expression of FOXL2.<sup>9</sup> Moreover, FOXL2 has been linked to steroid metabolism, detoxification of reactive oxygen species, inflammatory processes, and carcinogenesis, in addition to its involvement in the pathogenesis of BPES.<sup>9-12</sup>

The presence of mutations in the coding region of FOXL2 (88%) has been found to be associated with human developmental disorders, particularly those affecting the eyes.<sup>8,13</sup> Within the BPES cohort, it has been observed that 81% of genetic defects are intragenic mutations that disrupt the protein

function of FOXL2. These mutations include missense changes, frameshift and nonsense mutations, in-frame deletions, and duplications.<sup>14-16</sup> In addition, a 7.4kb deletion in the distal cis-regulatory region (283 kb 5'-upstream to FOXL2) has been identified as causing the loss of promoter-enhancer contact, resulting in reduced expression of FOXL2 in the BPES family.<sup>17</sup> Nevertheless, a comprehensive understanding of the correlation between mutations in cis-regulatory elements and the pathogenesis of BPES has yet to be established.

In the present study, our investigation uncovers a previously unreported occurrence of polydactyly in BPES, which is exclusively observed in affected males. Moreover, a 255-bp-deletion in the BPES patients has been successfully identified in close proximity (556-bp 5'-upstream to transcription start site). This deleted fragment displays a diverse array of active histone modifications and significantly enhances the promoter activity of FOXL2. Collectively, our findings demonstrate the identification of a unique deletion within the FOXL2 promoter, leading to a distinctive manifestation within a type II BPES family. This underscores the significance of conducting genetic screening for cis-regulatory elements in heritable diseases.

## METHOD

### Patient

This study investigated a consanguineous three-generation family affected by BPES, with all patients displaying early onset of the condition. The ophthalmologist conducted clinical examinations and confirmed the presence of clinical features. The proband (III:3), a 5-year-old boy, inherited the pathogenic allele from his father. All patients exhibited common characteristics of BPES, such as a small palpebral fissure, eyelid ptosis, epicanthus inversus, and telecanthus. Notably, polydactyly was observed exclusively in male BPES patients (III-3, II-2, and II-6), while it was absent in female BPES individuals (I-2 and II-4). The father underwent two-stage blepharoplasty surgeries and an additional finger excision during the 1990s. In accordance with the principles outlined in the Declaration of Helsinki, informed consent for research was obtained from all participants or their legal guardians. The utilization of clinical samples with patient consent was granted approval by the Institutional Research Ethics Committee (approval No. SH9H-2019T185-2).

### DNA Extraction and Polymerase Chain Reaction

Blood samples were collected from the family under study, and genomic DNA was extracted from the leukocytes of peripheral venous blood using the method previously described.<sup>8</sup> For mutation analysis, the promoter region of FOXL2 was amplified using PCR (Forward primer: 5'-GAAATCTGCCG GTACTCGCT-3'; Reverse primer: 5'-TCCCTCAGCCTGATGTTTGTC-3'). The PCR reaction mixture consisted of 200 ng genomic DNA, 50 µl 2× GC-rich buffer, 16 µl of a dNTP (2.5 mmol/L), 2 U LA Taq (Takara Biotechnology (Dalian) Co., Ltd), 4 µl (10 µmol/L) of each primer, and ddH<sub>2</sub>O to a final volume of 100 µl. The PCR amplification protocol consisted of the following steps: an initial denaturation at 95°C for 2 minutes, followed by 40 cycles of denaturation at 95°C for 60 seconds, annealing at 63°C for 30 seconds, and extension at 72°C for 30 seconds. A final elongation step was performed at 72°C for 3 minutes. The resulting PCR products were purified and subjected to sequencing in both forward and reverse directions using an ABI 3730 DNA sequencer to validate the presence of mutations.

### Whole Exome Sequencing

The Illumina NextSeq500 platform was utilized for conducting whole exome sequencing (WES). Library preparation was carried out following the manufacturer’s guidelines for the Agilent SureSelect v6 kit. The alignment of sequence reads to the UCSC hg38 reference genome, indexing of the reference genome, variant calling, and annotation were accomplished using a Burrows-Wheeler Alignment-based pipeline.

### Luciferase Reporter Assay

FOXL2-expressed Chinese Hamster Ovarian cells were maintained in a 1640 medium supplemented with 10% fetal calf serum and 1% penicillin/streptomycin. Luciferase assays were performed using the pGL3-basic Reporter System (Promega), following previously described methods.<sup>2</sup> A total of 3\*10<sup>4</sup> Chinese Hamster Ovarian cells were plated in 500 ml of culture medium per well in 24-well plates. The cells were then incubated with plasmids in Opti-MEM media (Gibco-Invitrogen) for 12 h. Subsequently, the media was replaced with fresh media, and the cells were further incubated for 48 h. After a brief centrifugation to remove cell debris, 20 µl of cell lysate was used to measure luciferase activity on a Lumimark luminometer (Bio-Rad Laboratories, Hercules, CA, USA).

## RESULTS

### Clinical Features

All individuals within this consanguineous three-generation BPES family exhibited typical clinical manifestations of eyelid malformation, including small palpebral fissures, ptosis, telecanthus, and epicanthus inversus (Fig. 1A and B). Remarkably, in addition to the aforementioned eyelid symptoms, all male patients (III-3, II-2, and II-6) presented with a history of preaxial polydactyly, a condition that was not observed in female BPES individuals (I-2 and II-4). Notably, all polydactyly patients displayed an additional thumb, which was connected through a rudimentary soft tissue pedicle (Fig. 1C). Significantly, among the family members unaffected by BPES (I-1, II-7, and III-4), none exhibited polydactyly. In addition, both I-2 and II-4 displayed regular menstrual cycles, normal ovarian functions, and fertility. Consequently, we deduced that this particular family manifests type II BPES with polydactyly, a condition exclusively observed in male patients.

### Identification of a Novel Regulatory Element Deletion (Chr3: 138947694-138947948 del) in a Chinese Family with BPES type II

To elucidate the genetic basis of the family, WES was conducted on individuals II-6 and III-3, with individual II-5 serving as a control (Fig. 1D). Through analysis of the shared mutations in II-6 and III-3, a range of germline mutations were identified and are presented in Supplemental Table 1, Supplemental Digital Content 1, <http://links.lww.com/SCS/F582>. However, none of these mutations exhibit any association with BPES or polydactyly. Given that mutations in cis-regulatory elements can contribute to the development of BPES, we proceeded to clone and sequence a neighboring regulatory element of FOXL2. Consequently, individuals affected by BPES exhibited 2 alleles: a pathogenic allele and a wild-type (WT) allele. Conversely, unaffected individuals solely displayed a WT allele (Fig. 2A). Based on the findings of Sanger’s sequencing, the specific localization of the Chr3: 138,947,694-138,947,948 del mutation has been identified in individuals diagnosed with BPES (Fig. 2B). Notably, this mutation was

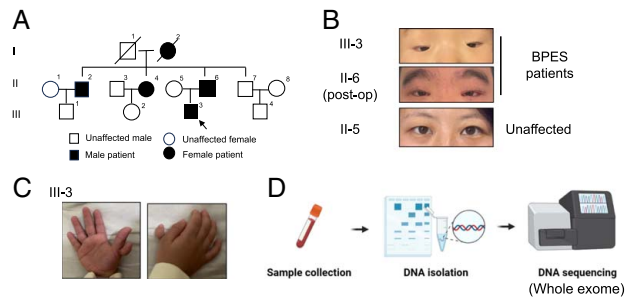


**FIGURE 1.** The clinical manifestations of the BPES within this particular family. (A) The pedigrees of the BPES cases that were included in the study, with affected individuals denoted by closed symbols and the proband indicated by an arrow. The generations are represented by Roman numerals, while individual numbers are represented by Arabic numerals. (B) The facial photographs of both affected and unaffected individuals within the family. (C) Photographs of the polydactyly presentation of the family. (D) Schematic diagrams illustrating the flowchart of the whole exome sequencing assays for testing germline mutations in this family. BPES indicates blepharophimosis-ptosis-epicanthus inversus syndrome; PCR, polymerase chain reaction.

absent in both healthy individuals and the dbSNP database (<http://www.ncbi.nlm.nih.gov/SNP>), indicating its potential as a pathogenic variant.

### The Deletion Leads to Decreased Promoter Activity

To gain a deeper understanding of the regulatory role of the deleted region, we proceeded to map this specific area within the FOXL2 promoter locus. This investigation revealed that the deleted region exhibited a notable presence of active histone modification markers, namely H3K4me1, H3K4me3, and H3K27Ac (Fig. 3A). To further validate the regulatory function of this region, we subsequently cloned the reverse sequence of a 1021-bp DNA fragment located upstream of the FOXL2 transcription start site (Chr3:138,947,161-138,948,182, WT group), as well as the Chr3: 138,947,694-138,947,948 del group (MT group). Both wild-type (WT) and mutant (MT) fragments were inserted into the pGL3-basic vector to conduct the luciferase reporter assay (Fig. 3B). The findings revealed that the WT fragment exhibited a substantial 3.2-fold increase in signal intensity compared with the control group with an empty vector. Conversely, the MT group displayed a significant reduction in luminance intensity compared with the WT group, albeit slightly higher than the empty group (Fig. 3C). Collectively, these outcomes suggest that the deletion within the regulatory element may lead to compromised FOXL2 promoter activity.

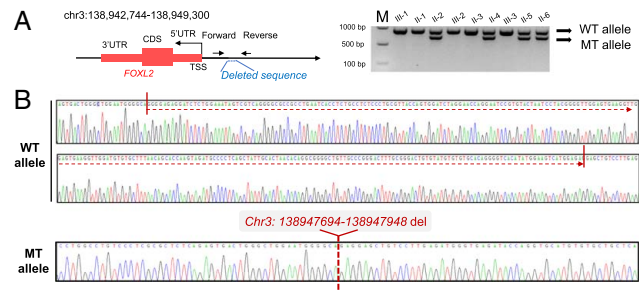


**FIGURE 2.** The PCR products of BPES patients and unaffected family members. (A) Gel electrophoresis of the PCR products from the BPES patients revealed 2 fragments of 931 and 676 bp. The unaffected individuals contained a single fragment of 931 bp. (B) The sequence is further analyzed by Sanger’s sequencing. BPES indicates blepharophimosis-ptosis-epicanthus inversus syndrome; MT, mutant type; WT, wild-type.

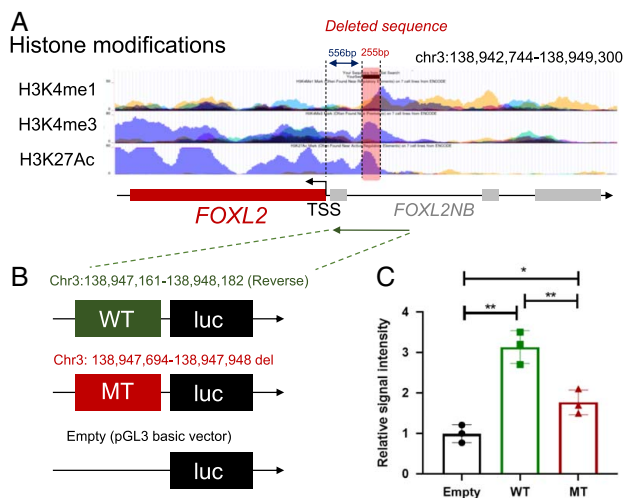


**FIGURE 3.** Analysis of the promoter activity of deleted fragments. (A) The deleted fragment is in an active regulatory region of FOXL2, with several active histone modifications; this figure is drawn by UCSC genome browser (<https://genome.ucsc.edu/cgi-bin/hgTracks>). (B) As reflected by the luciferase activity in CHO cell, the deletion of Chr3: 138,947,694-138,947,948 reduces the signal intensity. Statistically significant differences are indicated by \*  $P < 0.05$ , \*\*  $P < 0.01$ . Measured by unpaired, two-tailed students t-test. CHO indicates Chinese Hamster Ovarian; FOXL2, forkhead box L2; MT, mutant type; WT, wild-type.

### DISCUSSIONS

Winged helix/forkhead transcription factors such as FOXL2 play a key role in the early development of eyelid and female gonads in vertebrate species.<sup>3,10,17</sup> Globally, more than 200 FOXL2 mutations have been identified in patients suffering from BPES.<sup>6</sup> Most studies have noticed that mutations in the coding region could result in the abrogation of FOXL2 functions; however, only limited studies have revealed that the regulatory elements of FOXL2 are involved in the pathogenesis of BPES. Notably, a 7.4 kb deletion in the distal cis-regulatory region abrogates the normal promoter-enhancer interaction, which also leads to the pathogenesis of BPES.<sup>17</sup> In this study, we showed a 255-bp-deletion in the promoter area of FOXL2 could also lead to BPES type II, highlighting the importance of genetic screening of regulatory elements in heritable diseases.

Polydactyly has not been documented in BPES, to the best of our knowledge. It is noteworthy that we initially reported a family with BPES type II, where only affected males exhibited polydactyly. Importantly, FOXL2 plays a crucial role in sex determination and may contribute to sex-specific phenotypes.<sup>18-20</sup> However, this hypothesis necessitates further comprehensive investigations.

Furthermore, it is noteworthy to mention that various anomalies of the eyelids are also linked to notable abnormalities of the fingers. For instance, Smith-Magenis Syndrome, which is caused by the retinoic acid-induced 1 gene, can manifest with both eyelid manifestations (telecanthus, ptosis) and polydactyly.<sup>21-23</sup> Furthermore, Fraser syndrome is characterized by the concurrent presence of eyelid fusion and polydactyly.<sup>24,25</sup> Notably, a recent case study documented the occurrence of brachydactyly in a 7-year-old girl with BPES. Genetic analysis confirmed the absence of FOXL2 coding region mutations in this patient,<sup>26</sup> aligning with our WES data. These findings suggest a strong correlation between the development of the eyelid and the finger. While the association between this FOXL2 promoter deletion and finger development remains unknown, further studies are necessary to ascertain the correlation between this genetic variant and the sexually biased phenotype.

### CONCLUSIONS

In the present study, we have successfully identified a 255-bp-deletion in the BPES patients located in close proximity. This deleted fragment exhibits a diverse range of active histone modifications and significantly contributes to the promoter activity of FOXL2. Furthermore, our investigation reveals a previously unreported manifestation of polydactyly in BPES, exclusively observed in affected males. Consequently, our study contributes valuable insights into the genotype-phenotype associations of the FOXL2 protein, emphasizing the crucial significance of genetic screening of cis-regulatory elements in the evaluation of hereditary disorders.

### REFERENCES

- Zhou J, Jiang X, Wu H, et al. Dissecting the fate of Foxl2-expressing cells in fetal ovary using lineage tracing and single-cell transcriptomics. *Cell Discov* 2022;8:139
- Li F, Chen H, Wang Y, et al. Functional studies of Novel FOXL2 variants in chinese families with blepharophimosis-ptosis-epicanthus inversus syndrome. *Front Genet* 2021;12:616112
- Chai P, Li F, Fan J, et al. Functional analysis of a novel FOXL2 indel mutation in Chinese families with blepharophimosis-ptosis-epicanthus inversus syndrome type I. *Int J Biol Sci* 2017;13:1019-1028
- Chacon-Camacho OF, Salgado-Medina A, Alcaraz-Lares N, et al. Clinical characterization and identification of five novel FOXL2 pathogenic variants in a cohort of 12 Mexican subjects with the syndrome of blepharophimosis-ptosis-epicanthus inversus. *Gene* 2019;706:62-68
- Nabih O, Arab L, El Maaloum L, et al. Bilateral cataract in a child with blepharophimosis-ptosis-epicanthus inversus syndrome: a surgical challenge. *Int J Surg Case Rep* 2022;92:106845
- Wang Y, Wu Q, Cao W, et al. Clinical and genetic studies of 17 Han Chinese pedigrees and 31 sporadic patients with blepharophimosis-ptosis-epicanthus inversus syndrome. *Mol Vis* 2022;28:352-358
- Kaur I, Hussain A, Naik MN, et al. Mutation spectrum of forkhead transcriptional factor gene (FOXL2) in Indian Blepharophimosis Ptosis Epicanthus Inversus Syndrome (BPES) patients. *Br J Ophthalmol* 2011;95:881-886
- Fan J, Zhou Y, Huang X, et al. The combination of polyalanine expansion mutation and a novel missense substitution in transcription factor FOXL2 leads to different ovarian phenotypes in blepharophimosis-ptosis-epicanthus inversus syndrome (BPES) patients. *Hum Reprod* 2012;27:3347-3357
- Tucker EJ. The genetics and biology of FOXL2. *Sex Dev* 2022;16:184-193
- Dai S, Qi S, Wei X, et al. Germline sexual fate is determined by the antagonistic action of dmrt1 and foxl3/foxl2 in tilapia. *Development* 2021;148:1-14
- Du H, Guo Y, Wu X, et al. FOXL2 regulates the expression of the Col4a1 collagen gene in chicken granulosa cells. *Mol Reprod Dev* 2022;89:95-103
- Herman L, Legois B, Todeschini AL, et al. Genomic exploration of the targets of FOXL2 and ESR2 unveils their implication in cell migration, invasion, and adhesion. *FASEB J* 2021;35:e21355
- Bouman A, van Haelst M, van Spaendonck R. Blepharophimosis-ptosis-epicanthus inversus syndrome caused by a 54-kb microdeletion in a FOXL2 cis-regulatory element. *Clin Dysmorphol* 2018;27:58-62
- Kim JH, Bae J. Differential apoptotic and proliferative activities of wild-type FOXL2 and blepharophimosis-ptosis-epicanthus inversus syndrome (BPES)-associated mutant FOXL2 proteins. *J Reprod Dev* 2014;60:14-20
- Bertho S, Pasquier J, Pan Q, et al. Foxl2 and its relatives are evolutionary conserved players in gonadal sex differentiation. *Sex Dev* 2016;10:111-129
- Decock CE, Shah AD, Delaey C, et al. Increased levator muscle function by supramaximal resection in patients with blepharophimosis-ptosis-epicanthus inversus syndrome. *Arch Ophthalmol* 2011;129:1018-1022

17. D'Haene B, Attanasio C, Beysen D, et al. Baere, Disease-causing 7.4 kb cis-regulatory deletion disrupting conserved non-coding sequences and their interaction with the FOXL2 promoter: Implications for mutation screening. *PLoS Genet* 2009;5:e1000522
18. Elzaat M, Jouneau L, Thepot D, et al. High-throughput sequencing analyses of XX genital ridges lacking FOXL2 reveal DMRT1 up-regulation before SOX9 expression during the sex-reversal process in goats. *Biol Reprod* 2014;91:153
19. Hersmus R, Kalfa N, de Leeuw B, et al. FOXL2 and SOX9 as parameters of female and male gonadal differentiation in patients with various forms of disorders of sex development (DSD). *J Pathol* 2008;215:31–38
20. Uhlenhaut NH, Jakob S, Anlag K, et al. Somatic sex reprogramming of adult ovaries to testes by FOXL2 ablation. *Cell* 2009;139:1130–1142
21. Babovic-Vuksanovic D, Jalal SM, Garrity JA, et al. Visual impairment due to macular disciform scars in a 20-year-old man with Smith-Magenis syndrome: another ophthalmologic complication. *Am J Med Genet* 1998;80:373–376
22. Chen RM, Lupski JR, Greenberg F, et al. Ophthalmic manifestations of Smith-Magenis syndrome. *Ophthalmology* 1996;103:1084–1091
23. MarianneJensen L, Kirchoff M. Polydactyly in a boy with Smith-Magenis syndrome. *Clin Dysmorphol* 2005;14:189–190
24. Takamiya K, Kostourou V, Adams S, et al. A direct functional link between the multi-PDZ domain protein GRIP1 and the Fraser syndrome protein Fras1. *Nat Genet* 2004;36:172–177
25. Das D, Modaboyina S, Raj S, et al. Clinical features and orbital anomalies in Fraser syndrome and a review of management options. *Indian J Ophthalmol* 2022;70:2559–2563
26. Zhou L, Wang T, Wang J. Blepharophimosis ptosis epicanthus inversus syndrome with congenital hypothyroidism and brachydactyly in a 7-year-old girl. *Ophthalmic Plast Reconstr Surg* 2017;33:S82–S84

OPEN

## Incidence of Ventriculomegaly in Patients With Craniosynostosis

Baihui Liu, PhD, Jun Li, MSc, Songchunyan Zhang, MSc, Yueqing Wang, MSc, and Chenbin Dong, MD

From the Shanghai Key Laboratory of Birth Defect, Key Laboratory of Neonatal Disease, Department of Pediatric Surgery, Children's Hospital of Fudan University, Shanghai, China.

Received July 29, 2023.

Accepted for publication August 26, 2023.

Address correspondence and reprint requests to Chenbin Dong, MD, Key Laboratory of Neonatal Disease, Department of Pediatric Surgery, Children's Hospital of Fudan University, Ministry of Health, 399 Wan Yuan Road, Shanghai 201102, China; E-mail: dcb426@163.com

The authors report no conflicts of interest.

This work was supported by the Natural Science Foundation of Shanghai (Grant No. 22ZR1408300).

**Supplemental Digital Content is available for this article. Direct URL citations are provided in the HTML and PDF versions of this article on the journal's website, [www.jcraniofacialsurgery.com](http://www.jcraniofacialsurgery.com).**

This is an open access article distributed under the terms of the Creative Commons Attribution-Non Commercial-No Derivatives License 4.0 (CCBY-NC-ND), where it is permissible to download and share the work provided it is properly cited. The work cannot be changed in any way or used commercially without permission from the journal. Copyright © 2023 The Author(s). Published by Wolters Kluwer Health, Inc. on behalf of Mutaz B. Habal, MD.

ISSN: 1049-2275

DOI: 10.1097/SCS.00000000000009805

**Abstract:** Hydrocephalus is variously associated with syndromic craniosynostosis (CS), while it is randomly encountered in nonsyndromic CS. But actually, the ventriculomegaly in CS is less described. In this study, the authors aim to establish whether ventriculomegaly is common in patients with CS, in both syndromic and nonsyndromic. Retrospective measurements of Evans index (EI) were taken from thin-section computed tomography scans of 169 preoperative CS patients to assess cerebral ventricular volume. EI > 0.3 indicates ventricular enlargement. A total of 169 CS patients who underwent computed tomography scan from February 2018 to December 2021 were retrospectively evaluated, including 114 males and 55 females. The average age at diagnosis was 16 months (range: 1–103 mo). Among them, 37 with syndromic CS, including 17 ventricular megal patients, had an EI > 0.3 (46.0%), and 4 of them had intracranial hypertension and needed ventriculoperitoneal shunt treatment before cranial vault remodeling. One hundred and thirty-two had nonsyndromic CS (100 single-suture CS, 32 multisuture CS), and 26 of them had an EI of 0.3 or greater (19.7%). Ventricular megal is common among patients with CS. Early craniotomy may stabilize ventricular dilation.

**Key Words:** Craniosynostosis, Evans index, incidence, ventriculomegaly

Craniosynostosis (CS) is a common developmental deformity of the skull in children, characterized by premature ossification and fusion of the skull sutures. It occurs in 1 in 2500 newborns. In addition to the craniofacial deformity, some children may also be complicated by serious central nervous system dysplasia, such as hydrocephalus and Chiari deformity. Hydrocephalus is commonly observed in children with syndrome CS and is one of the indications for surgery. However, we discovered that a portion of patients already exhibit ventricular dilation despite the absence of intracranial hypertension at the first visit to the hospital. The aim of this study was to evaluate the incidence of ventricular dilation in children with CS and provide new insight into it.

## METHODS

### Participants

Medical and imaging records of 169 patients with CS at the Children's Hospital of Fudan University between January 2018 and December 2022 were collected. All patients underwent computed tomography (CT) with 3-dimensional reformatted images to confirm CS at first diagnosis, and patients with conditions such as brain atrophy or developmental abnormalities were excluded.

### Measurements

The Evans index (EI) was used to describe the degree of ventricular dilation, which is defined as the ratio of the maximal width of the frontal horns to the maximum inner skull diameter. The width was measured on 3 consecutive axial slices, and the slice with the largest diameter at the maximal width of the frontal horns was selected.<sup>1</sup> The normal range for the EI is between 0.2 and 0.25, a ratio between 0.25 and 0.30 represents early or questionable enlargement, and a value > 0.3 indicates significant ventricular enlargement.<sup>2</sup>